

Saturated Optical Absorption by Slow Molecules in Hollow-Core Photonic Band-Gap Fibers

Jan Hald* and Jan C. Petersen

Danish Fundamental Metrology Ltd., Matematiktorvet 307, DK-2800 Kgs. Lyngby, Denmark

Jes Henningsen

Niels Bohr Institute, Universitetsparken 5, DK-2100 Copenhagen Ø, Denmark

(Received 12 January 2007; published 25 May 2007)

We report on saturated absorption in a hollow-core photonic band-gap fiber filled with $^{12}\text{C}_2\text{H}_2$ molecules. We find that slow molecules provide a major contribution to the signal in the limit of low optical power and low pressure where the signal deviates significantly from the usual Lorentzian line shape. In particular, we observe a linewidth reduction of about 3 times as compared to the transit-time limited linewidth.

DOI: [10.1103/PhysRevLett.98.213902](https://doi.org/10.1103/PhysRevLett.98.213902)

PACS numbers: 42.70.Qs, 33.70.Jg, 39.30.+w, 42.62.Fi

The realization of gas-filled hollow-core photonic band-gap (HC-PBG) fibers has opened a class of spectroscopic investigations in which weak molecular transitions can be studied at high optical intensity [1–5]. In previous experiments, the collisions between the molecules and the inner wall of the fiber limited the coherence time resulting in broadened spectroscopic line shapes and thus reduced resolution. We demonstrate that this effect can be reduced in saturated absorption spectroscopy by careful choice of the experimental parameters.

The idea of saturated absorption is to eliminate the Doppler contribution to the linewidth by selecting molecules which move at right angle to two counter-propagating optical beams [6]. Having accomplished this, a residual contribution to the linewidth originates from the finite interaction time t of molecules moving across the interaction region with thermal velocities, since by a Fourier transform argument, this causes a linewidth contribution of $\sim 1/t$. The transit-time limited linewidth (HWHM) is given by [6] $\Delta\nu \approx 0.2\bar{u}/w_0$, where \bar{u} is the average molecular speed and w_0 is the beam radius of the Gaussian-shaped optical beam profile. The theory for transit-time limited saturation spectroscopy as developed 30 years ago [7] suggested that it was possible to reach linewidths below the transit-time limit by favoring the slow molecules of the Maxwell-Boltzmann distribution. Subsequent experimental work [8–10] supported this conclusion, which can be understood as follows. The resonant interaction causes the molecule to undergo Rabi oscillations between the two states coupled by the field. The frequency of these oscillations is proportional to the optical field strength, and saturation sets in when a full Rabi cycle can be completed before the coherence of the interaction is destroyed. Spontaneous decay can be neglected for the long-lived states considered, and the intermolecular collision rate can be reduced by lowering the pressure, leaving the transit-time as the dominant coherence limiting mechanism. By reducing the optical intensity, we may now arrive at a situation where mainly the slow molecules contribute

to the saturation signal, since they are the only molecules which can complete a Rabi cycle before leaving the interaction region.

Previous work [8–10] was concerned with free-space configurations, where the transit-time is defined by the time it takes a molecule to cross the Gaussian-shaped laser beam, and experiments were performed on strong fundamental vibration transitions of CH_4 and OsO_4 . In this Letter, we explore the same ideas in a different wavelength regime, for a weaker type of transition, and in a radically different experimental configuration. We have chosen to work with C_2H_2 (acetylene), which has been used for saturated absorption in HC-PBG fibers previously [3–5]. Furthermore, acetylene is included in the CIPM (International Committee for Weight and Measures) list of recommended radiations for the practical realization of the metre [11]. It is the only molecule included which has absorption lines within the $1.5\ \mu\text{m}$ telecommunication wavelength band, and it is important to study the factors that limit the precision with which the recommended wavelength can be realized. The interpretation of our results, however, is generally applicable to other molecules as well.

For molecules inside the core of a HC-PBG fiber, the interaction region is limited by the core diameter, and in experiments performed so far, the linewidth has indeed been at or above the transit-time limited linewidth [1–5]. This indicates that wall collisions are as detrimental to the coherent interaction between the molecule and the optical field as would be a complete removal of the molecule. The dimensionless parameters of interest are [10] $\eta = \gamma w_0/u$ and $\theta = \Omega w_0/u$, where γ is the intermolecular collision rate, w_0 is the beam radius of the optical mode, u is the most probable molecular speed, and Ω is the angular Rabi frequency. Thus, η is the ratio between the intermolecular collision rate and the wall collision rate and θ is the ratio between the Rabi frequency and the wall collision rate. The intermolecular collision rate for the acetylene P9 line has been measured at high pressure ($p \gtrsim 0.1\ \text{kPa}$) [12,13]:

$\gamma = 2\pi(45 \text{ kHz/Pa})p$, where p is the acetylene pressure. We use the same value here, although the collisional broadening coefficient may differ at our lower pressure [14]. The $1/e^2$ optical mode radius in the HC-PBG fiber is specified to $w_0 = 5.3 \mu\text{m}$. For $^{12}\text{C}_2\text{H}_2$ at room temperature, we find $u = 435 \text{ m/s}$. The Rabi frequency can be expressed as $\Omega = \Gamma\sqrt{P/P_{\text{sat}}}$, where P and P_{sat} are the optical power and the saturation power and Γ is the molecular decay rate. The saturation power for the P9 line in an equivalent fiber has been measured to 23 mW [3]. In those measurements, the decay rate was dominated by the wall collisions and hence $\Gamma = u/w_0$. Thus, the dimensionless parameters representing the pressure and pump power are given by $\eta = 3.4 \times 10^{-3} \text{ Pa}^{-1}p$ and $\theta = \sqrt{P/23 \text{ mW}}$. Four different regimes can be identified [8,10]. $\theta \ll \eta \ll 1$: All saturated molecules experience intermolecular collisions before wall collisions and η determines the linewidth given by [7] $\Delta\nu_{\text{HWHM}} = 1.51\eta^{1/2}u/(2\pi w_0)$. $\eta \ll \theta \ll 1$: Molecules with radial velocity $u_r \lesssim \theta u$ are saturated and the linewidth is determined by θ . $\eta \ll 1 \ll \theta$: The transit-time limited regime where all molecules are saturated and the linewidth scales as [8] $\sim u/w_0[1 + (P/P_{\text{sat}})]^{1/2}$. $1 \ll \eta$: Intermolecular collisions dominate for all velocities and transit-time effects can be neglected.

The experimental setup is shown in Fig. 1. An Extended Cavity diode Laser (ECL) is used to seed two 60 mW Erbium Doped Fiber Amplifiers (EDFA). A stable Fabry-Perot (FP) resonator provides the frequency scale when scanning the ECL. The output of the pump EDFA is coupled into free space with collimating lens L1. The output of the probe EDFA goes via the fiber-coupled acousto-optical modulator (AOM) and is coupled to free space with lens L4. Variable neutral density filters (ND1, ND2) and wave plates (λ_1 and λ_2) are used to adjust the pump and probe power and polarization. The pump beam is modulated at 1.3 kHz by a mechanical chopper (CH). The AOM shifts the probe frequency by 30 MHz and adds a 100% amplitude modulation to the probe at a frequency of 70 Hz. The HC-PBG fiber is produced by Crystal Fibre A/S

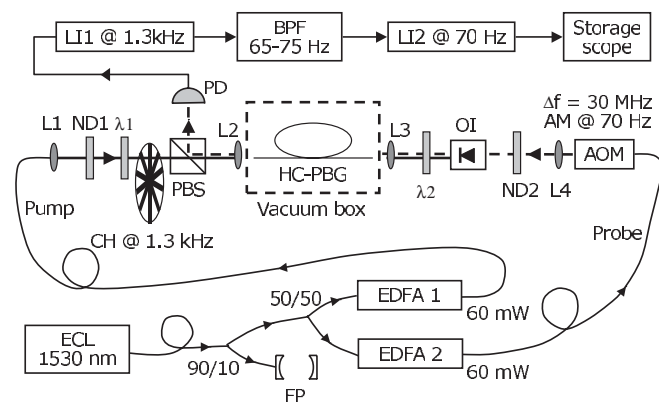


FIG. 1. Schematic diagram of the main components in the setup.

(type designation CF-0133, 10 μm nominal core diameter) and is placed in a vacuum box, which can be filled with acetylene. The fiber length is either 12 cm, 105 cm or 8 m. At each pressure, we chose the fiber length that makes the resonant acetylene absorption closest to 50%. The pump and probe light is coupled into the HC-PBG fiber through antireflection coated windows in the vacuum box using focusing lenses L2 and L3. The optical isolator OI prevents coupling of pump light back into the EDFA. The polarizing beam splitter (PBS) reflects the probe onto the photo detector PD. A double lock-in detection scheme is used with lock-in amplifiers LI1 and LI2. The first lock-in detection at 1.3 kHz separates the saturated absorption signal from the Doppler background [6]. The 30 MHz frequency shift of the probe eliminates the interference signal between the probe and residual reflection of the modulated pump from lens L2 and vacuum box windows. The 70 Hz amplitude modulation of the probe and the second stage lock-in detection (L2) eliminate the direct signal from the residual pump reflections. A Band Pass Filter (BPF) with a 65 Hz–75 Hz transmission window between LI1 and LI2 is used for further noise reduction. The averaging time constant for LI2 is set to 30 ms with a 24 dB/octave slope. The signal is acquired while scanning the laser across the P9 line in $^{12}\text{C}_2\text{H}_2$ at 1530.3710 nm. The scan rate at low pressure and low intensity is about 5 MHz/s. All results are obtained with an average probe power of 10 μW in the fiber.

In Fig. 2 (trace (a)), we show an example of a measured saturated absorption signal. Trace (b) in Fig. 2 is the residual from a Lorentzian fit to trace (a). It is obvious that the saturated absorption signal is too peaked at the line center for a Lorentzian fit, in agreement with theory [7,10].

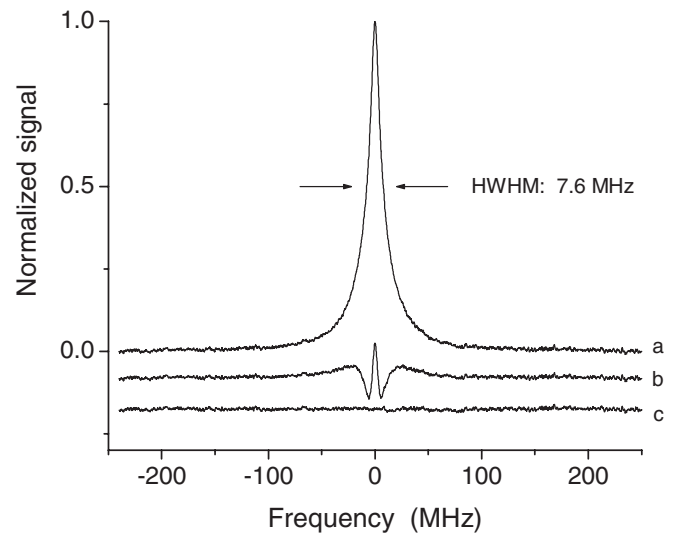


FIG. 2. (a) Saturated absorption signal. Pump power: 100 μW ($\theta = 0.07$). Acetylene pressure: 3 Pa ($\eta = 0.01$). Number of averaged scans: 280. (b) Residual after a Lorentzian fit. (c) Residual after a double Lorentzian fit. The residuals are displaced vertically for clarity.

Trace (c) in Fig. 2 is the residual from a double Lorentzian fit to trace (a), i.e., a fit to the equation

$$y = a_1/(1 + \Delta^2/\Gamma_1^2) + a_2/(1 + \Delta^2/\Gamma_2^2), \quad (1)$$

with a_1 , a_2 , Γ_1 , and Γ_2 as free parameters and Δ as the detuning. This empirical line shape fits the data well with $a_1/a_2 = 1.3$, $\Gamma_1 = 4.5$ MHz and $\Gamma_2 = 16.3$ MHz. The large fraction of weakly saturated fast molecules contributes with a broad line shape due to their high wall collision rate. The small fraction of slow molecules provides a signal of similar amplitude due to a higher degree of saturation, but this contribution has a smaller width due to low collision rate. We find that the normal Lorentzian fit is just as good as the double Lorentzian fit for measurements at either $\theta \geq 1$ or $\eta \geq 1$.

The HWHM linewidth of the saturated absorption signal as a function of normalized Rabi frequency θ is shown in Fig. 3 for $\eta = 0.01$. At high pump power ($\theta \geq 1$), the linewidth has only a weak dependence on the pump power and is characterized by the transit-time limited linewidth of about 23 MHz as found previously [3]. The smallest observed linewidth is 7.0 MHz at $\theta = 0.065$, i.e., a reduction by more than a factor of 3 below the transit-time limited linewidth. The data at $\theta < 0.4$ appear to have a linear dependence on θ , and the linewidth extrapolated to $\theta = 0$ is 5.8 MHz. The inset shows theoretical data [10] for $\eta = 0.04$ together with measured data at $\eta = 0.03$. The difference in slope for the theoretical and experimental data can be explained by the uncertainty in our determination of θ . The discrepancy at $\theta = 0$ is possibly caused by the use of a collisional broadening coefficient measured at much higher pressure or experimental conditions not included

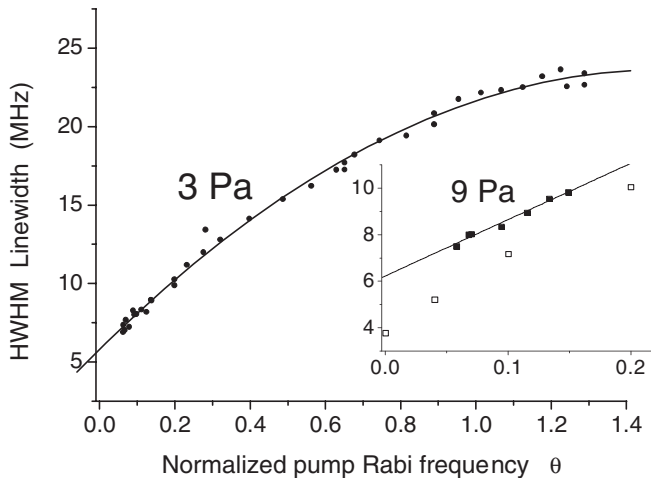


FIG. 3. Filled circles: Measured HWHM linewidth as a function of θ . Acetylene pressure: 3 Pa ($\eta = 0.01$). Solid line: Empirical quadratic fit for extrapolation to $\theta = 0$. Open squares (inset): Theoretical data from [10], Fig. 9, for $\eta = 0.04$. Filled squares (inset): Measurements at 9 Pa ($\eta = 0.03$) with a linear extrapolation. The data in the inset have the same units as the main plot.

in the theory, e.g., attenuation of pump and probe beams along the fiber, assumptions on molecular collisions [14,15], the small deviation from a Gaussian mode due to a fraction of the field located outside the hollow-core, as well as weak surface modes [16].

In Fig. 4, we plot the HWHM linewidth extrapolated to $\theta = 0$ (as in Fig. 3) versus the normalized pressure η . The linewidth at $\eta \geq 1$ is about 30% above the theoretical value [7]. At lower pressure, the difference between theory and experiment is larger, and the experimental values seem to reach a minimum linewidth of about 5.6 MHz. Besides the explanations given above, the extrapolation to $\theta = 0$ may be less accurate at lower pressure.

Although the linewidth can be reduced significantly at low pressure and low power, it is for many practical applications important to consider the signal-to-noise ratio as well. All our measurements are acquired with the same scan time and time constants, and we can therefore use the standard deviation σ of the residual after a double Lorentzian fit (see Fig. 2) as our noise measure. We correct for multiple scans so that σ is the standard deviation of the residual for a single scan normalized to the amplitude of the saturated absorption signal. In Fig. 5 we show σ as a function of θ for the same 3 Pa data as in Fig. 3. The noise increases rapidly at $\theta \leq 0.1$ because the saturated fraction of molecules becomes very small. The small noise increase at $\theta \geq 0.3$ is caused by the increased amount of pump light reflected from lens L2 and vacuum windows. One potential application of saturated absorption in a HC-PBG fiber is as the reference in optical frequency standards. The slope of the first derivative of the signal at the line center can be used as the error signal in the laser frequency stabilization feedback loop. This slope depends on the signal close to the line center where the contribution from the slow molecules is largest. In Fig. 5, we have included the slope

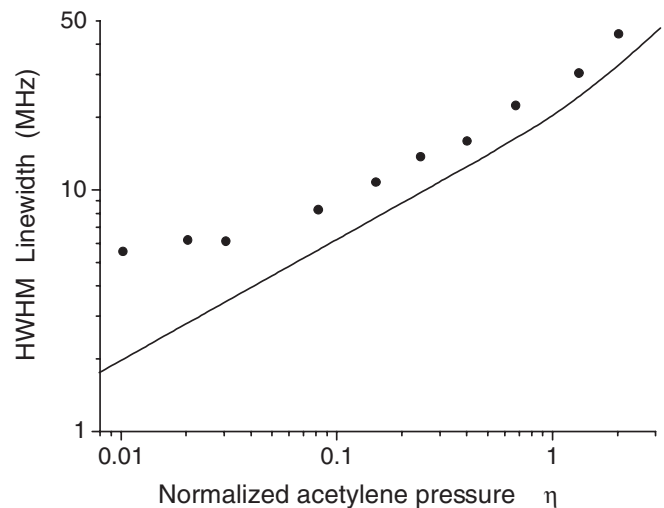


FIG. 4. Measured HWHM linewidth extrapolated to $\theta = 0$ as a function of pressure. The solid line shows the theoretical linewidths [7].

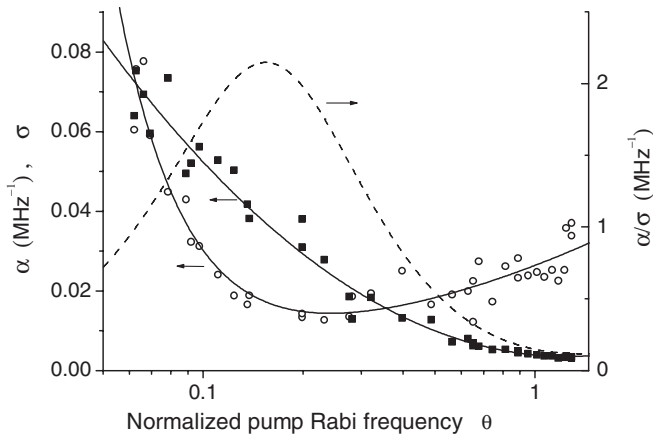


FIG. 5. Open circles: Standard deviation σ of the residual after a Double Lorentzian fit to the saturated absorption signal. Solid squares: Calculated slopes α at the center of the first derivatives of the Double Lorentzian fits. α and σ are normalized to the amplitude of the saturated absorption signal. Solid lines: Empirical fits to α and σ data. Dashed line: Ratio between α and σ fits. All data correspond to the 3 Pa data in Fig. 3.

normalized to the signal amplitude (α) calculated from the double Lorentzian fits to the saturated absorption signal. In particular, we see that the slope increases by a factor of 20 when going from $\theta \approx 1$ to $\theta = 0.065$. The fact that the first derivative is influenced much more by lowering pressure and intensity than the saturated absorption line itself has been discussed previously [10]. The stability of a frequency standard is determined by the ratio between the slope of the error signal and the noise level in the detection. The ratio α/σ is shown in Fig. 5 as the dashed line, and it shows that the optimal working point for our 8 m HC-PBG fiber filled with 3 Pa acetylene is at $\theta = 0.15$, corresponding to about 500 μW average pump power or less than 3% of the saturation power.

The first derivative of the absorption signal can be realized in, e.g., FM spectroscopy with a modulation frequency much larger than the linewidth [17] or in low frequency wavelength modulation spectroscopy with a small modulation amplitude. The noise contribution from the pump reflections can be reduced in an improved setup or by optimizing the probe power. If we assume the noise is completely independent of the pump power and hence σ is simply proportional to the inverse of the measured saturated absorption signal amplitude, we find that the maximum for α/σ occurs at $\theta = 0.45$, i.e., still well below the saturation power. It is remarkable that the optimum pump power appears to be smaller than the saturation power. This allows for efficient stabilization of low power lasers like diode lasers or fiber lasers. In an integrated device, where the HC-PBG fiber is sealed by splicing to a single mode fiber, the high loss in the splice (up to 10 dB [5]) is a minor problem when so low power is needed.

In conclusion, we have shown that for saturated absorption in a HC-PBG fiber, the regime at low pressure and low optical intensity offers reduced linewidths and increased resolution. With an actively stabilized laser, it will be possible to further decrease the power in order to test the theory in the $\theta < 0.05$ range. Possible applications include secondary optical frequency standards as well as high resolution spectroscopy of closely spaced lines. Although our experiments employ acetylene, it is important to stress that nothing in the interpretation is specific to this molecule. The conclusions are equally valid for any molecule for which transit-time limited saturated absorption can be observed in a HC-PBG fiber, for example, HCN [3].

We acknowledge C. Chardonnet for his comments, Crystal Fibre A/S for providing the fiber, and the Danish Research Council for Technology and Production Sciences for financial support under Project No. 26-04-0177 Advanced optical fibre technology: novel concepts and applications.

*Electronic address: jha@dfm.dtu.dk

- [1] F. Benabid, F. Couny, J. C. Knight, T. A. Birks, and P. St. J. Russel, *Nature (London)* **434**, 488 (2005).
- [2] S. Ghosh, J.E. Sharping, D.G. Ouzounov, and A.L. Gaeta, *Phys. Rev. Lett.* **94**, 093902 (2005).
- [3] J. Henningsen, J. Hald, and J.C. Petersen, *Opt. Express* **13**, 10475 (2005).
- [4] R. Thapa, K. Knabe, M. Faheem, A. Naweed, O.L. Weaver, and K.L. Corwin, *Opt. Lett.* **31**, 2489 (2006).
- [5] F. Couny, P.S. Light, and F. Benabid, and P. St. J. Russell, *Opt. Commun.* **263**, 28 (2006).
- [6] W. Demtröder, *Laser Spectroscopy* (Springer, Berlin, 1996).
- [7] C.J. Bordé, J.L. Hall, C.V. Kunasz, and D.G. Hummer, *Phys. Rev. A* **14**, 236 (1976).
- [8] S.N. Bagaev, A.E. Baklanov, A.S. Dychkov, P.V. Pokasov, and V.P. Chebotayev, *Pis'ma Zh. Eksp. Teor. Fiz.* **45**, 371 (1987) [*JETP Lett.* **45**, 471 (1987)].
- [9] S.N. Bagayev, A.E. Baklanov, V.P. Chebotayev, and A.S. Dychkov, *Appl. Phys. B* **48**, 31 (1989).
- [10] C. Chardonnet, F. Guernet, G. Charton, and C. Bordé, *Appl. Phys. B* **59**, 333 (1994).
- [11] R. Felder, *Metrologia* **42**, 323 (2005).
- [12] W.C. Swann and S.L. Gilbert, *J. Opt. Soc. Am. B* **17**, 1263 (2000).
- [13] M. Kusaba and J. Henningsen, *J. Mol. Spectrosc.* **209**, 216 (2001).
- [14] M.H. Wappelhorst, M. Mürtz, P. Palm, and W. Urban, *Appl. Phys. B* **65**, 25 (1997).
- [15] G. Buffa, S. Carocci, A. Di Lieto, P. Minguzzi, F. Quochi, O. Tarrini, and M. Tonelli, *Phys. Rev. Lett.* **74**, 3356 (1995).
- [16] K. Saitoh, N. A. Mortensen, and M. Koshiba, *Opt. Express* **12**, 394 (2004).
- [17] G.C. Bjorklund, M. D. Levensen, W. Lenth, and C. Ortiz, *Appl. Phys. B* **32**, 145 (1983).